JOURNAL OF MAGNETIC RESONANCE **127,** 1–16 (1997)
ARTICLE NO. MN971184

Measurement of Homonuclear Cross-Correlation Cross-Relaxation Rates along an Effective Field: Application to Dipole–Dipole Cross-Correlation

Hervé Desvaux*

Center for Interdisciplinary Magnetic Resonance, National High Magnetic Field Laboratory, 1800 East Paul Dirac Drive, Tallahassee, Florida 32310

Received January 10, 1997; revised April 7, 1997

We describe three new schemes to explore homonuclear cross-correlation contributions to relaxation along an effective field tilted by an angle θ from the static magnetic field direction. Their key feature is to detect, during the evolution time t_1, multiquantum transverse coherences whose frequencies are characteristic of the multispin order produced by cross-correlation processes. This makes it possible to obtain in-phase magnetization in both dimensions. The three schemes correspond to the combination of two evolutions due either to static J coupling in the transverse plane or to cross-correlation cross-relaxation along an effective field. This combination allows the conversion of one-spin order into multispin order and the reverse. If only cross-correlation cross-relaxation transfers are involved, there is no restriction on the coupling network. The quantitative exploitation of the results to obtain structural information from cross-correlation-induced relaxation rates requires a normalization coefficient which is provided by the simultaneous monitoring of one-spin coherence. These ideas have been tested experimentally in the case of dipole–dipole cross-correlation on a sample of cyclosporin. Buildup curves at various angles θ are described which yield information on the internal dynamics. © 1997 Academic Press

Key Words: **cross-correlation; relaxation; multiquantum; multispin orders; spectral density.**

I. INTRODUCTION

Relaxation theory is a second-order time-dependent perturbation theory (*1*), which makes use of the correlation function of a randomly varied Hamiltonian at different times. Most of the time, this random Hamiltonian $H_1(t)$ is the sum of different terms, and depending on their tensorial character, cross-correlation terms can or cannot be present (*2–8*). In the following, we will refer to cross-correlation-induced relaxation simply as cross-correlation. For a diamagnetic sample composed of spins $\frac{1}{2}$, the two kinds of interactions between which cross-correlation may appear are dipole–dipole (DD) and chemical shift anisotropy (CSA). This requires that the two interactions considered have one common spin. We will use the following notation: cross-correlation between two dipolar interactions will be DD/DD, and that between one dipolar and CSA interaction will be CSA/DD.

Although cross-correlation has been described theoretically in NMR for more than 30 years (*2–6*), very few methods have been suggested and tested experimentally for measuring cross-correlation rates (*9, 10*), and there have been few publications on their use for the exploration of structural or dynamic properties of molecules (*11, 12*). Starting from this surprising observation, we have tried to understand why measuring cross-correlation rates presents difficulties.

First of all, the largest effect induced by cross-correlations is on the evolution of transverse magnetizations (*13*). It results in a different width for each line of a multiplet (*8, 13*), an effect which has been called ''differential line broadening'' (*14*), or in the observation of extra cross-peaks in COSY experiments (*15*). The strong chemical shift anisotropy on nuclei other than protons gives rise to nonnegligible cross-correlation (*10*), and several experiments have been suggested to measure heteronuclear transverse self-relaxation rates ($1/T_2$) without artifacts from CSA/DD cross-correlation (*16–19*). However, because of uncertainties in the coupling network, the homogeneity, the phase of the spectrum, the noise level, etc., it is difficult from standard transverse relaxation measurements to extract reliable values for the cross-correlation rates.

For relaxation along an effective field, cross-correlation leads most of the time to a change in the number of spins involved in the coherence. We will refer to these cross-relaxation processes as cc-cross-relaxation in contrast with the ac-cross-relaxation where only auto-correlation functions are involved. The easiest way to measure the cc-cross-relaxation rates consists therefore in turning longitudinal n-spin order coherences into n quantum coherences combined with a n-quantum filter. This has been done in DQF- (*20*) and TQF-NOESY (*21*) experiments, which allow the measurement of the transformation of longitudinal one-spin order

* Present address: Laboratoire Commun de R.M.N., Service de Chimie Moléculaire, C.E.A. Saclay, F-91191 Gif sur Yvette, France.

1090-7807/97 $25.00

into two- (respectively three) spin order due to the CSA/DD (DD/DD, respectively) cross-correlation. This filtering always gives rise to an antiphase spectral pattern in the dimension F2. The main drawback of this approach is the presence in the spectrum of zero-quantum cross peaks (*20, 21*). In large molecules where $\omega\tau_c \gg 1$, cc-cross-relaxation rates, which only depend on $J(\omega)$, are negligible compared to the other relaxation rates which also depend on $J(0) \gg J(\omega)$ (*8, 22, 23*). This difficulty has been overcome by the use of off-resonance RF irradiation (*24*), which appears for measuring cc-cross-relaxation as a mandatory request, which we call R1. Longitudinal relaxation measurements have also been used for the heteronuclear case, where it is possible to obtain in-phase cross peaks through a refocusing delay as a result of the large difference of resonance frequencies and to the large and nearly constant $^1J_{HX}$ scalar coupling values (*25–27*). The same approach can be used for the homonuclear case, through selective spin-lock irradiation and selective transfer (*28*), but the remote couplings may influence the measurement (*29*) and a very high magnetic field is then required (*30*).

The theoretical expressions of cc-cross-relaxation rates show that they contain structural information (see below). In particular, DD/DD cc-cross-relaxation rates depend on the angle sustained by the two pairs of spins and on the internuclear distances. Such an angular constraint would represent a large improvement for structure determination, since this information can only be determined through triangulation by NOESY-like experiments when the three spins are not coupled. In such a case, the Karplus law (*31*) does not hold. This angular information seems to be particularly relevant for large deuterium-labeled proteins for which the structural information is only obtained from the amide protons and the triangulation becomes very difficult (*32, 33*). One should however notice that in a buildup curve, the initial slope is proportional to $\kappa \cdot I_0$, where κ is the cross-relaxation rate and I_0 is the ''diagonal'' peak magnetization at $\tau_m = 0$. Only relative structural constraints can thus be determined if the normalization coefficient I_0 is not measured.

At this stage, it becomes possible to summarize the other desirable conditions for measuring cross-correlation cross-relaxation rates:

—Obtaining in-phase cross peaks in both dimensions (R2a) would be a nice feature since it would facilitate the quantitative integration of the signal. Moreover the integration procedure allows one to circumvent the inconveniences associated with zero-quantum cross peaks, whose absence (R2b) is desirable but not always possible.

—The determination of the normalization factor (R3) during the same acquisition time would be a valuable advantage for structural purposes.

—It is necessary to obtain spectra where it is possible to assign the two or three spins involved in a given cross-correlation even if the coupling network contains more spins (R4).

—The pulse sequence should work even in the absence of scalar coupling between the spins (R5).

Keeping in mind these requirements (R1–R5), we have tried to inductively design new schemes to measure cc-cross-relaxation rates. Their key ideas are based on the following remarks:

(i) During the evolution time t_1 of a 2D experiment, one can simultaneously acquire the transverse evolution of multiquantum coherences of different orders (*34, 35*), for example, single and triple quantum. The single-quantum peak intensity gives access to the normalization coefficient (R3). The evolution of multiquantum coherences induces in-phase cross peaks in the dimension F1 (R2a), and their resonance frequencies are characteristic of the involved protons (R4). Finally multiquantum transverse coherences do not require scalar coupling between the involved spins (R5).

(ii) It is possible to transform multiquantum coherences into multispin order along an effective field axis (R1) through $\pi/2$ hard pulses and off-resonance RF irradiation with adiabatic rotations (*36*).

(iii) During the time t_2, one acquires only single-quantum coherences, but only single-quantum–one-spin order coherences at $t_2 = 0$ yield nonvanishing integrals (R2a, R2b).

Combining these three ideas results in the design of pulse sequences. They should allow the transformation of magnetization from its thermal equilibrium value to multiquantum transverse coherences during the evolution time t_1 and back to one quantum for the acquisition time t_2. The conversion (or the reverse process) of one-spin order into multispin order can be obtained either by the transverse evolution under the influence of the static scalar coupling Hamiltonian (we label this evolution process J) or by the longitudinal relaxation evolution under the influence of cross-correlation (label δ). We name each sequence with the succession (α–β) of the two-evolution process which creates α and back converts β multiquantum coherences. The three possible sequences which allow the study of cc-cross-relaxation are δ–J, J–δ, and δ–δ.

This article is organized as follows. The expressions of the relaxation rates along an effective field axis are first given in the case of n homonuclear spins. For the experimental application, we focus on dipole–dipole cross-correlation and describe the three sequences with experimental illustrations. We finally discuss their relative advantages and drawbacks.

II. THE RELAXATION RATES

A. Expressions of the Relaxation Rates

We consider a spin system composed of n homonuclear spins $\frac{1}{2}$ (typically protons), called I^k, whose Larmor fre-

quency is ω. These spins experience a strong off-resonance RF irradiation whose amplitude is $2\omega_1$ and frequency $\omega + \Delta$. We consider the relaxation of any spin order coherence along the effective field axis *OZ* due to dipolar and CSA interactions. The effective field makes an angle θ with the static magnetic field *Oz* (*37*):

$$\tan\theta = \frac{\omega_1}{\Delta}. \qquad [1]$$

The effective field amplitude Ω in the rotating frame is

$$\Omega = \sqrt{\Delta^2 + \omega_1^2}. \qquad [2]$$

The RF field amplitude ω_1 and the offset Δ are assumed to be sufficiently large to allow the neglect of all offset effects due to the dispersion of proton chemical shifts. We consequently consider only one angle θ for all protons (*37*). In this section, we summarize all relaxation rates expressions in the case of dipolar and axially symmetric CSA relaxation along the effective field axis *OZ*. We assume that the overall correlation time τ_c is small enough for the condition $\Omega\tau_c \ll 1$ to be fulfilled. This means that τ_c is shorter than about 100 ns (*38*). We have derived most of these expressions from those published (*8, 22, 23, 28, 37*). The other relaxation rates have been computed through the classical procedure using the master equation of relaxation and the Wigner matrices (*39*) for easy computations of the changes of representation (see Refs. (*8, 22, 35, 37, 38*) for examples of relaxation rate computation). To express the relaxation rates in term of spectral density values an assumption on the normalization of the second rank irreductible tensors $T_{2,m}$ is required. We choose

$$\forall m,\ \mathrm{Tr}(T_{2,m}T_{2,m}^{\dagger}) = \tfrac{1}{4}.$$

1. Self-relaxation rates. We note all self-relaxation rates as $\rho^{abc\cdots}$ where the exponent $abc\cdots$ means that it is the self relaxation of the $m+1$ multispin order $2^m I_Z^a I_Z^b I_Z^c \cdots$. We obtain this self-relaxation rate by decomposing the random Hamiltonian $H_1(t)$ into a sum of terms, each representing an interaction, either the CSA interaction of one spin or the dipole–dipole interaction between two spins. Each pair of interaction terms represents an elementary contribution. In fact, for dipolar and CSA interactions, no cc-self-relaxation contribution exists (this result is obtained by the same analysis as described below). $\rho^{abc\cdots}$ is then a sum of elementary ac-self-relaxation rates. We note each elementary contribution as $\rho_\beta^{abc\cdots}$, where $abc\cdots$ represents the spin order as described previously, and β represents the interaction: $\beta = a, b$ means the dipolar interaction between I^a and I^b, $\beta = a$ means the chemical shift anisotropy on proton I^a. The number of elementary self-relaxation rates can be determined by noting first that the CSA interaction depends on one spin only whereas the dipolar interaction depends on two spins, and second that the master equation of relaxation contains double commutators involving the coherence under study and the two interaction terms. As a consequence, CSA interaction on spin I^k would contribute to relaxation of the coherence $2^m I_Z^a I_Z^b I_Z^c \cdots$ only if $k \in \{a, b, c, \cdots\}$. Otherwise the double commutators vanish, since operators of different spins commute. Moreover the commutation property of the different spins allows a factorization in the double commutators of the master equation of all spins different from I^k. The elementary self-relaxation rate $\rho_k^{abc\cdots}$ is then equal to ρ_k^k. We thus have

$$\rho_k^{abc\cdots} = 0 \quad \text{if } k \notin \{a, b, c, \cdots\} \qquad [3a]$$

$$\rho_k^{abc\cdots} = \rho_k^k \quad \text{if } k \in \{a, b, c, \cdots\}. \qquad [3b]$$

We can also compute the elementary self-relaxation rate $\rho_{k,l}^{abc\cdots}$ of $2^m I_Z^a I_Z^b I_Z^c \cdots$ due to the dipole–dipole interaction between I^k and I^l:

$$\rho_{k,l}^{abc\cdots} = 0 \quad \text{if } k \notin \{a, b, c, \cdots\} \text{ and } l \notin \{a, b, c, \cdots\} \qquad [4a]$$

$$\rho_{k,l}^{abc\cdots} = \rho_{k,l}^k \quad \text{if } k \in \{a, b, c, \cdots\} \text{ and } l \notin \{a, b, c, \cdots\} \qquad [4b]$$

$$\rho_{k,l}^{abc\cdots} = \rho_{k,l}^l \quad \text{if } k \notin \{a, b, c, \cdots\} \text{ and } l \in \{a, b, c, \cdots\} \qquad [4c]$$

$$\rho_{k,l}^{abc\cdots} = \rho_{k,l}^{kl} \quad \text{if } k \in \{a, b, c, \cdots\} \text{ and } l \in \{a, b, c, \cdots\}. \qquad [4d]$$

All elementary self-relaxation rates can be expressed in terms of ρ_k^k, $\rho_{k,l}^k$, and $\rho_{k,l}^{kl}$. These three rates have the following expressions:

• For the dipolar relaxation rates of one spin order I_Z^k due to dipolar interaction between spins I^k and I^l,

$$\rho_{k,l}^k = (\tfrac{1}{3} + \tfrac{1}{2}\sin^2\theta)J_{k,l}(0) + (1 + \tfrac{1}{2}\sin^2\theta)J_{k,l}(\omega) + (2 - \sin^2\theta)J_{k,l}(2\omega), \qquad [5]$$

where $J_{k,l}$ is the dipolar spectral density associated to the dipolar interaction between I^k and I^l.

• The self-relaxation rate of one-spin order I_Z^k due to chemical shift anisotropy relaxation on spin I^k is

$$\rho_k^k = \tfrac{8}{3}\sin^2\theta J_k(0) + 2(\cos^2\theta + 1)J_k(\omega), \qquad [6]$$

where J_k is the spectral density associated to the chemical shift anisotropy of spin I^k.

• Finally the dipolar self-relaxation rate of two-spin order terms $2I_Z^kI_Z^l$ due to the I^k–I^l dipolar interaction is

$$\rho_{k,l}^{kl} = 3\sin^2\theta\cos^2\theta J_{k,l}(0) + (4\cos^4\theta - 3\cos^2\theta + 1)J_{k,l}(\omega) + (1-\cos^4\theta)J_{k,l}(2\omega). \quad [7]$$

The self-relaxation rate expression of any spin order is obtained by considering all elementary contributions and using Eqs. [3] and [4]. The general expression of the self-relaxation rate of the m-spin order term $2^mI_Z^aI_Z^bI_Z^c\cdots$ is

$$\rho^{abc\cdots} = \sum_{k\in\{a,b,c,\cdots\}}\ \sum_{l\notin\{a,b,c,\cdots\}} \rho_{k,l}^{k} + \sum_{\substack{(k,l)\in\{a,b,c,\cdots\}\\ k<l}} \rho_{k,l}^{kl} + \sum_{k\in\{a,b,c,\cdots\}} \rho_k^k. \quad [8]$$

If we consider a large number of spins, Eq. [8] shows that self-relaxation rates generally increase with the number of coherences involved in the longitudinal spin order.

2. Cross-relaxation rates. We note the cross-relaxation rates between $2^mI_Z^aI_Z^bI_Z^c\cdots$ and $2^{m'}I_Z^{a'}I_Z^{b'}I_Z^{c'}\cdots$ as $\sigma_{abc\cdots}^{a'b'c'\cdots} = \sigma_{a'b'c'\cdots}^{abc\cdots}$. The same decomposition of the random Hamiltonian $H_1(t)$ and the same exploration of the possible contribution to cross-relaxation can be performed for cross-relaxation as was described for self-relaxation. We do not detail it and we give directly the result. All elementary cross-relaxation rates depend only on the following three. The dipolar ac-cross-relaxation rate between one-spin order terms I_Z^k and I_Z^l due to the dipolar interaction between I^k and I^l is

$$\sigma_{k,l} = (\sin^2\theta - \tfrac{1}{3})J_{k,l}(0) + \sin^2\theta J_{k,l}(\omega) + 2\cos^2\theta J_{k,l}(2\omega). \quad [9]$$

The dipolar cc-cross-relaxation rate between one I_Z^k and three $4I_Z^lI_Z^kI_Z^m$ spin order terms due to the dipolar interactions between the two pairs $I^k - I^l$ and $I^k - I^m$ is

$$\delta_{k,lkm} = 3\sin^2\theta\cos^2\theta J_{k,lkm}(0) + (4\cos^4\theta - 3\cos^2\theta + 1)J_{k,lkm}(\omega) + \sin^2\theta(1+\cos^2\theta)J_{k,lkm}(2\omega), \quad [10]$$

where $J_{k,lkm}$ is the Fourier transform of the dipole–dipole cross-correlation function between $I^k - I^l$ and $I^k - I^m$. Finally, the CSA/DD cc-cross-relaxation rate between one I_Z^k and two $2I_Z^kI_Z^l$ spin order terms due to dipolar interaction between I^k and I^l and chemical shift anisotropy on I^k is

$$\delta_{k,kl} = -4\sin^2\theta\cos\theta J_{k,kl}(0) - 4\cos^3\theta J_{k,kl}(\omega), \quad [11]$$

where $J_{k,kl}$ is the Fourier transform of the CSA–dipole cross-correlation function.

All cross-relaxation rates can be expressed by linear combinations of these three rates. We successively express the cross-relaxation rates $\sigma_{abc\cdots}^{a'b'c'\cdots}$ between $2^mI_Z^aI_Z^bI_Z^c\cdots$ and $2^{m'}I_Z^{a'}I_Z^{b'}I_Z^{c'}\cdots$ as a function of the difference of spin order $|m'-m|$.

• For $m'-m=0$, if the two coherences $2^mI_Z^aI_Z^bI_Z^c\cdots$ and $2^mI_Z^{a'}I_Z^{b'}I_Z^{c'}\cdots$ do not have $(m-1)$ common spins, the cross-relaxation rate $\sigma_{abc\cdots}^{a'b'c'\cdots}$ vanishes; otherwise,

$$\sigma_{abc\cdots}^{a'bc\cdots} = \sigma_{a,a'} + \sum_{k\in\{b,c,\cdots\}} \delta_{k,aka'}. \quad [12]$$

• For $|m'-m|=1$, and assuming without loss of generality $m'>m$, $\sigma_{abc\cdots}^{a'b'c'\cdots}$ does not vanish only if the two coherences have m common spins. The rate expression is then

$$\sigma_{abc\cdots}^{a'abc\cdots} = \sum_{k\in\{a,b,c,\cdots\}} \delta_{k,ka'}. \quad [13]$$

• For $|m'-m|=2$, and choosing as above $m'>m$, $\sigma_{abc\cdots}^{a'b'c'\cdots}$ does not vanish only if the two coherences have m common spins. The rate expression is then

$$\sigma_{abc\cdots}^{a'b'abc\cdots} = \sum_{k\in\{a,b,c,\cdots\}} \delta_{k,a'kb'}. \quad [14]$$

• Finally for $|m'-m|>2$, the cross-relaxation rate $\sigma_{abc\cdots}^{a'b'c'\cdots}$ always vanishes.

For a large spin system, the cross-relaxation rates (Eqs. [12]–[14]) generally increase with the number of spins involved in the longitudinal spin order. It results that the validity of initial slope approximation in a buildup curve should hold for a shorter time for high number spin order than for one-spin order.

B. Correlation Function Expressions

1. General expression. It has already been shown that the expressions of ac-self- and ac-cross-relaxation rates as a function of the spectral densities are general, when the dipolar or CSA interactions do not have any static contribution to the Hamiltonian (*1, 37*). The same result can be obtained for cc-cross-relaxation rates between two interactions of rank two.

We arbitrarily choose one of the two interactions and define it as the ''first'' interaction. We define the orientation in the molecular frame of the ''first'' interaction relative to the second as $\Omega_1 = (\theta_1, \phi_1)$. We define the orientation of the second interaction relative to the laboratory frame as

Ω_2. We call the second-rank tensorial products in the frame attached to the second interaction as $T'_{2,m'}$, and we call them $T_{2,m}$ in the laboratory frame. The ''first'' interaction can consequently be expressed as

$$H_1(t) = \sum_{m'=-2}^{2} \zeta_1 Y_{2,m'}(\Omega_1) T'_{2,m'} \quad [15]$$

$$= \sum_{m'=-2}^{2} \zeta_1 Y_{2,m'}(\Omega_1) \sum_{m=-2}^{2} D^2_{m',m}(\Omega_2) T_{2,m}, \quad [16]$$

where the ''first'' interaction has first been expressed in the frame attached to the ''second'' and then expressed in the laboratory frame. The $D^2_{m,m'}(\Omega)$ are the Wigner matrices of rank two, the $Y_{2,m}(\Omega)$ are the second-rank spherical harmonics, and $\zeta_{1,2}$ depends on the type of interaction considered (CSA or dipolar). Correlation functions can then be computed [1]:

$$G(\tau) = \sum_{m'=-2}^{2} \times \overline{\zeta_1(0)\zeta_2(\tau) Y_{2,m'}(\Omega_1(0)) D^2_{m,m'}(\Omega_2(0)) Y_{2,-m}(\Omega_2(\tau))}. \quad [17]$$

Finally the spectral density function is the Fourier transform of this function. Using this approach to compute the spectral density functions, we find that the coefficients in front of the spectral density values in the rate expressions are independent of the motional model. One may also notice that the sign of the cross-correlation spectral density values can be either positive or negative so that no preliminary guess can be made. This is in contrast to the case of the autocorrelation spectral density function.

2. Isotropic Brownian motion. We assume that the molecule undergoes a Brownian isotropic motion without distance variations. It is then described by a single correlation time τ_c. Under these conditions, the angle Ω_1 is constant and the term $Y_{2,m'}(\Omega_1(0))$ in the sum (Eq. [17]) can be factorized out. We must then consider the averaging of $D^2_{m,m'}(\Omega_2(0))Y_{2,-m}(\Omega_2(\tau))$. Using the properties of the Wigner matrices (*39*), these terms are different from 0 only if m' is equal to 0. We find, in agreement with previous published results (*8, 22, 23*), that the correlation function depends on $Y_{2,0}(\Omega_1) = (3\cos^2\theta_1 - 1)/2$. The different spectral density functions have the following expressions. The dipole spectral density function is

$$J_{k,l}(\omega) = \frac{3}{10} \frac{\gamma^4 \hbar^2}{r_{kl}^6} \frac{\tau_c}{1 + \omega^2 \tau_c^2}, \quad [18]$$

where γ is the magnetogyric ratio and r_{kl} the internuclear distance between spins I^k and I^l. The spectral density of the dipole–dipole cross-correlation is

$$J_{k,lkm}(\omega) = \frac{3}{10} \frac{\gamma^4 \hbar^2}{r_{kl}^3 r_{km}^3} \frac{3\cos^2\phi\widehat{_{lkm}} - 1}{2} \frac{\tau_c}{1 + \omega^2 \tau_c^2}, \quad [19]$$

where $\phi\widehat{_{lkm}}$ (previously called θ_1) is the angle between the vectors $\overrightarrow{I^k I^l}$ and $\overrightarrow{I^k I^m}$:

$$\cos^2\phi\widehat{_{lkm}} = \frac{(\vec{r}_{kl} \cdot \vec{r}_{km})^2}{r_{kl} r_{km}}. \quad [20]$$

The following comments can be made about the structural information provided by cross-correlation rates. In a triangle the description of the geometry requires three parameters out of the following six $\phi\widehat{_{lkm}}$, $\phi\widehat{_{klm}}$, $\phi\widehat{_{kml}}$, r_{kl}, r_{km}, and r_{lm}; they are not independent due to the relation between the three angles in a triangle. As a consequence a complete distance extraction through NOESY may be sufficient to characterize the triangle. However for many geometries, it may happen that one of the distances cannot be accurately determined because of spin-diffusion process or too large internuclear distances, and then the angle value becomes relevant. In any case, it is a useful check of the consistency of the distance extraction. Another potentially interesting feature of the structural information contained in cross-correlation cross-relaxation rates is that it allows a fast approximate characterization of the triangle shape from the sign of the spectral density function.

For an axially symmetric CSA tensor, the CSA spectral density function is

$$J_k(\omega) = \frac{1}{30} \omega^2 (\Delta\sigma_k)^2 \frac{\tau_c}{1 + \omega^2 \tau_c^2}, \quad [21]$$

where $\Delta\sigma_k$ is the chemical shift anisotropy on spin I^k. The spectral density of the CSA/DD cross-correlation is

$$J_{k,kl}(\omega) = \frac{1}{10} \omega \Delta\sigma_k \times \frac{\gamma^2 \hbar}{r_{kl}^3} \frac{3\cos^2\varphi_{k,kl} - 1}{2} \frac{\tau_c}{1 + \omega^2 \tau_c^2}, \quad [22]$$

where $\varphi_{k,kl}$ (previously called θ_1) is the angle between the vector $\vec{r}_{kl}$ and the axial direction of the CSA tensor on I^k. Cases of nonaxially symmetric CSA tensors can be treated in a similar manner (*8*).

3. Others types of motion. The analytical expressions of the spectral density functions for others types of motions require a motional model. Werbelow and Marshall (*40*) have considered the case of anisotropic Brownian motions in the

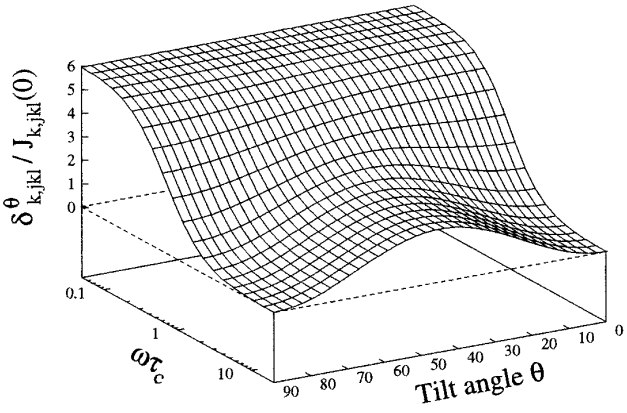

FIG. 1. Variation of the dipole–dipole cross-correlation cross-relaxation rates as a function of the angle θ and of the correlation time τ_c. An isotropic Brownian motion is assumed. As already observed (*24*), for large molecules the maximum of the cc-cross-relaxation rate is obtained for $\theta = 45°$ and the rate vanishes for $\theta = 0°$ and $\theta = 90°$.

case of dipole–dipole cross-correlation contributions to relaxation. In this model, the dipolar cc-cross-relaxation rate $\delta_{k,lkm}$ is no longer proportional to the second-rank Legendre polynomial of $\phi_{\widehat{lkm}}$, but also involves all second-order spherical harmonics. The cases of internal motions is particularly difficult to describe because the angle Ω_1 of Eq. [17] is not constant and furthermore its variation may be correlated to that of Ω_2.

Finally, a careful study of Eqs. [10] and [11] shows that the cross-correlation spectral density values at two (resp. three) frequencies of the CSA/DD (resp. DD/DD) cross-correlation can be determined at one static magnetic field, by measuring the cc-cross-relaxation rates at two (resp. three) different angles θ between the static and the effective field. This method of determination of spectral density values is an extension of that developped for dipolar ac-cross relaxation (*41*). As an example, Fig. 1 shows the variation of the dipole–dipole cc-cross-relaxation rate as a function of the angle θ for an isotropic Brownian motion.

III. EXPERIMENTAL PARAMETERS

All experiments have been carried out on samples of cyclosporin disolved in $CDCl_3$. Cyclosporin is a cyclic undecapeptide (MeBmt–Abu–Sar–MeLeu–Val–MeLeu–Ala–D-Ala–MeLeu–MeLeu–MeVal). The assignment of its proton resonances has been published (*42*), and its structure determined (*43*). The experimental temperature was 303 K. All spectra have been acquired on Bruker DMX300 spectrometers, either in a narrow- or a wide-bore magnet at 7 T. The spectrometers are equipped with three axes gradients, and the probeheads used are either a broadband inverse double channel or a broadband inverse triple channel. Many spectra were acquired by varying the different acquisition parameters in order to validate the experimental results, some (not shown since they have been acquired without off-resonance RF irradiation) have also been acquired on a Varian Unity*plus* operating at 720 MHz with a *z* gradient inverse triple-channel probehead.

Experiments to characterize the dynamic properties of the molecule have also been carried out. In particular, an average value of the correlation time per pair of protons has been determined using six 2D off-resonance ROESY matrices corresponding to six values of the angle θ (0°, 10°, 20°, 30°, 40°, and 47°) and one mixing time $\tau_m = 100$ ms. Using the procedure published in Ref. (*41*), at 303 K the average value of the correlation time per pair of protons was equal to 0.27 ns. Furthermore, diffusion processes have been explored to evaluate the possible loss of signal due to the use of encoding gradients. The principle was to compare spectra at various mixing times, τ_m, acquired by 1D selective off-resonance ROESY without encoding gradients and with encoding gradients (the latter is a straightforward modification of the GOESY sequence (*44*)). The ratio of diagonal peaks obtained by each sequence at each mixing time gives information concerning the signal loss by translational diffusion. Typically with a gradient of maximum amplitude 10 G applied for 1 ms, 50% of the signal is lost in 150 ms. The use of strong gradients to encode the signal should consequently be handled with care.

IV. DESCRIPTION OF THE SEQUENCES

For the experimental description, we focus on the dipole–dipole cross-correlation and disregard the CSA relaxation mechanism, since for proton nuclei in a field of 7 T it appears to be negligible. According to the schemes described in the Introduction, the relevant coherences during the evolution time should be the transverse triple-quantum coherences, since the DD/DD cross-correlation induces the creation of three-spin order from one-spin order. As already mentioned, there are two processes which enable the interconversion of single to triple quantum: either an evolution in the plane due to the *J*-coupling Hamiltonian, followed by hard pulses, or an evolution along an effective field axis under the influence of cross-correlation δ followed by the transformation of longitudinal three-spin order into triple quantum through hard pulses.

According to the schemes described in the Introduction, the reference experiment is the *J* coupling for creation and *J* coupling for detection. We have implemented this triple-quantum spectroscopy (TQS) sequence (Fig. 2) using encoding gradients and phase sensitive mode through time proportional phase increments (*45*). As a reference, a spectrum obtained with this sequence on cyclosporin is shown in Fig. 3. All cross peaks can be assigned using the published chemical shift data. One can notice that, due to proton equivalence

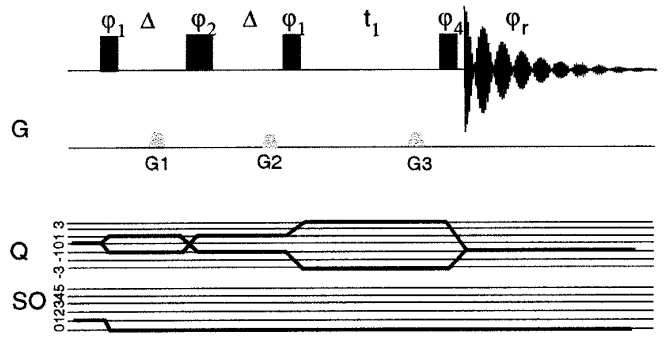

FIG. 2. Pulse sequence of the triple-quantum spectroscopy used in this article. The *G* line represents the gradient pulses, the *Q* lines the selected coherence pathway for −3 to +3 quantum. The *SO* line represents the longitudinal spin order, from 0 (transverse magnetization) to 5 longitudinal spin order. In the pulse sequence, the small (resp. large) filled boxes represent 90° (resp. 180°) hard pulses, and the duration Δ is chosen equal to $\frac{1}{4}J$. The gray half-ellipses represent encoding gradients. The values of $G1$, $G2$, and $G3$ are chosen so that $3 \cdot G3 = G1 - G2$. The phase of the hard pulses is as follows: ϕ_1 = 0°, 60°, 120°, 180°, 240°, 300°, 180°, 240°, 300°, 0°, 60°, 120°; ϕ_2 = 0°, 60°, 120°, 180°, 240°, 300°, 180°, 240°, 300°, 0°, 60°, 120°, 0°, 60°, 120°, 180°, 240°, 300°, 180°, 240°, 300°, 0°, 60°, 120°; ϕ_4 = 0°. The receiver phase ϕ_r is 0°, 180°, 0°, 180°, 0°, 180°, 180°, 0°, 180°, 0°, 180°, 0°. Finally phase-sensitive experiments are obtained by adding 30° to ϕ_1 and ϕ_2 every two FIDs.

(methyl) or strong coupling conditions, cross peaks can be present at frequencies in the ω_1 dimension other than the sum of the chemical shifts of the three partners (*46*). We successively consider the three sequences of cross-correlation exploration ($\delta-J$, $J-\delta$, and $\delta-\delta$). We will neglect the possible transformation of single-quantum-one-spin coherence into single-quantum-three-spin coherence through the effect of transverse evolution in the presence of cross-correlation (*15*). This effect, which induces relaxation-allowed cross peaks in COSY experiments (*15*), can always occur, but the rate of interconversion is on the order of δ (*47*) which is always much smaller than the *J* coupling values inducing resolved multiplets. The transverse evolution times we have used are always too small (between 10 and 360 ms for the acquisition) to observe transverse cross-correlation cross-relaxation rates smaller than typically 0.2 s^{-1}.

A. Creation by δ and Back Conversion by J Coupling

The $\delta-J$ sequence is represented in Fig. 4. The initial thermal equilibrium of the system is perturbed by the first pulse. Various choices can be made, either a simple 180° pulse or a saturation, such as that produced by a 90° hard pulse followed by a strong dephasing gradient. They produce different initial conditions. During the time τ_m, the spin system evolves under the influence of relaxation along an effective field axis tilted by the angle θ (Eq. [1]). The irradiation pulse is shaped such that adiabatic rotations bring the magnetization from the static magnetic field axis to the effective field axis and also bring them back (*36*). As the spin system evolves, all odd numbers of longitudinal spin orders are created through relaxation, in particular the three-spin order. The restriction to odd longitudinal spin order results from the assumption of purely dipolar relaxation. The 90° hard pulse converts these $2p + 1$-spin order coherences into multiquantum transverse coherences whose number is at most $2p + 1$, in particular triple-quantum transverse coherences for longitudinal three-spin orders (*34*). These transverse magnetizations are labeled in frequency during t_1 and converted back to single-quantum through the 90° pulse following t_1. The phase cycling of the hard pulse preceeding the evolution time allows one to select the triple-quantum transverse coherences. In this sequence, we can add encoding gradients to help select the triple-quantum coherences during t_1 and the single-quantum coherences after the last 90° hard pulse. Using the echo–antiecho scheme, a phase sensitive spectrum can be recorded.

In principle, this sequence is not very different from that proposed by Böhlen *et al.* (*48*) who also suggested starting from the creation of longitudinal multispin order. The difference resides in the detection. Their sequence was based on a Fourier transform on the phase of the first hard pulse of the filter which corresponds to the transformation of multispin order into single-quantum coherence.

Figure 5 shows a spectrum obtained with the $\delta-J$ sequence. The total experiment time was about 11 h. Many cross peaks are present and can easily be assigned through their resonance frequencies in both dimensions. This sequence does not allow one to acquire in-phase magnetization in the second dimension due to the dispersion of proton *J* coupling values which does not allow complete refocalization before acquisition. However no zero-quantum cross-peak transfer can occur, so that one can perform an integration in the magnitude mode. A comparison of the $\delta-J$ spectrum with the TQS spectrum shows that some cross peaks have disappeared. Using the $\delta-J$ sequence for short mixing times (condition of initial slope approximation), a cross peak at the frequency $(\omega_j + \omega_k + \omega_l, \omega_k)$ requires that *J* coupling values between I^j and I^k and between I^k and I^l do not vanish. The absolute cross-peak intensity is proportional to the sum of the cc-cross-relaxation rates: $\sigma^j_{jkl} + \sigma^k_{jkl} + \sigma^l_{jkl} = \delta_{j,kjl} + \delta_{k,jkl} + \delta_{l,jlk}$.

To check the consistency of the results, buildup curves have been measured for various angles θ. An example is given for $\theta = 0°$ (Fig. 6). Note that buildup curve behavior is regular. As theoretically predicted, no fluctuation due to the spin–spin coupling constants can be detected.

B. Creation by J Coupling, Back Conversion through Cross-Correlation

The second way explored was to create the triple-quantum coherences by *J*-coupling-induced transverse evolution, and

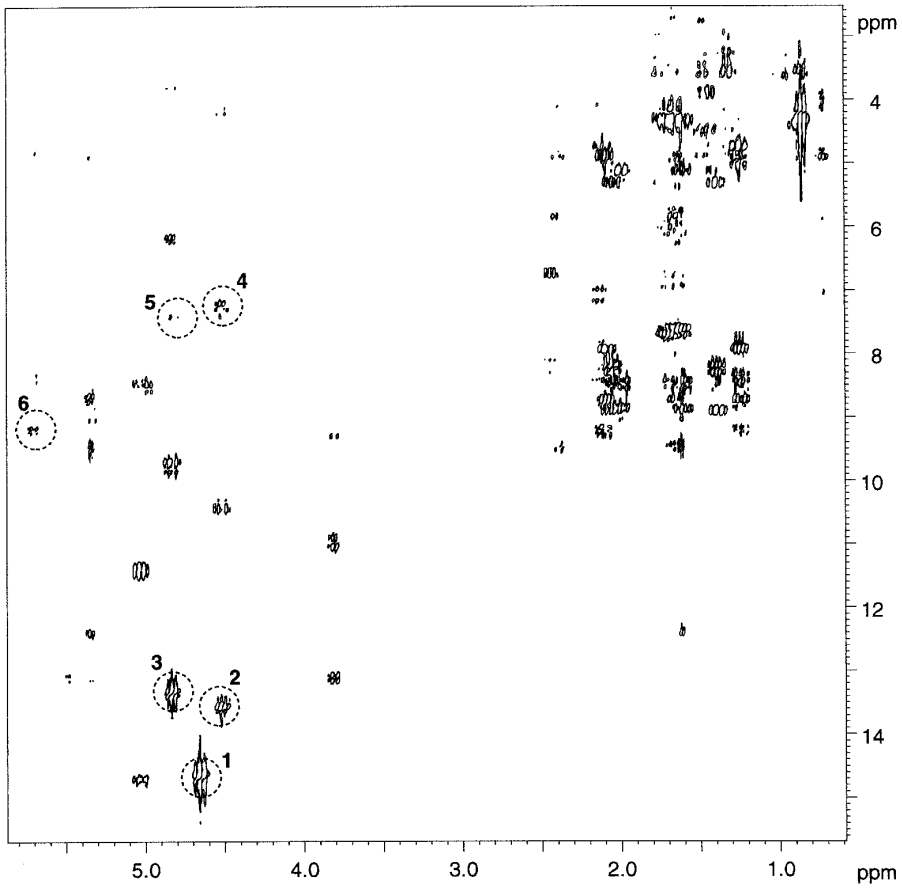

FIG. 3. TQS spectrum acquired with the sequence of Fig. 2. The experimental time was about 4 h, the duration Δ was chosen equal to 25 ms. The cross-peak amplitudes are of course dependent on this time. The six labeled cross peaks correspond respectively to the Val-5 ($H_N H_\alpha H_\beta$, H_α), Ala-7 ($H_N H_\alpha H_\beta$, H_α), D-Ala-8 ($H_N H_\alpha H_\beta$, H_α), Ala-7 ($H_\alpha H_\beta H'_\beta$, H_α), D-Ala-8 ($H_\alpha H_\beta H'_\beta$, H_α), and MeLeu-9 ($H_\alpha H_\beta H'_\beta$, H_α) interactions.

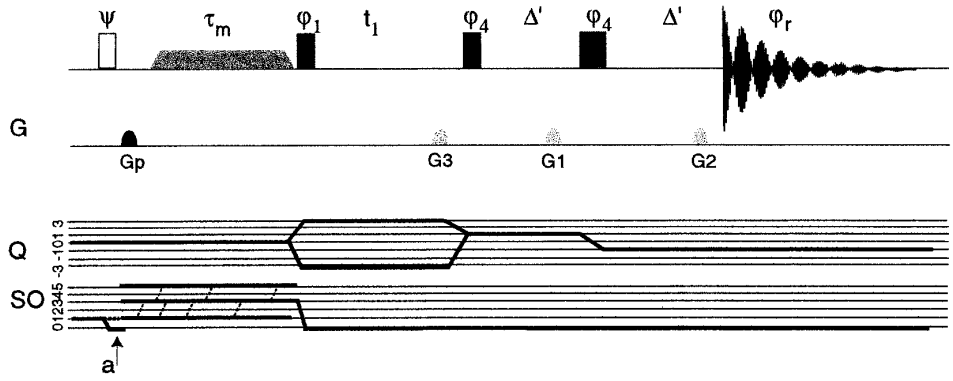

FIG. 4. Pulse sequence to explore dipole–dipole cross-correlation; three-spin order coherences are created by evolution under the influence of cross-correlation and converted to transverse triple-quantum coherences. The transverse three-spin order single-quantum coherence is detected through the transverse evolution due to scalar coupling. The same definitions as described in the legend to Fig. 2 are used. The nonfilled box represents the perturbing pulse. It could be either a saturation pulse or a 180° hard pulse; its phase ψ is set to 0°. The gray trapeze of duration τ_m represents the relaxation along an effective field axis with adiabatic rotation (*36*). The black half-ellipse *Gp* is a purging gradient, applied along a different axis than the coding gradients. The values of the encoding gradients are chosen so that $3 \cdot |G3| = G1 - G2$. By alternation of the sign of $G3$, a phase-sensitive experiment is obtained. Finally during the time τ_m all odd-spin order coherences are created through self-relaxation and ac- and cc-cross-relaxation. As a function of the choice of perturbing pulse, and as shown by the arrow labeled *a*, the buildup starts either from 0 or from $-I^k_{eq.}$.

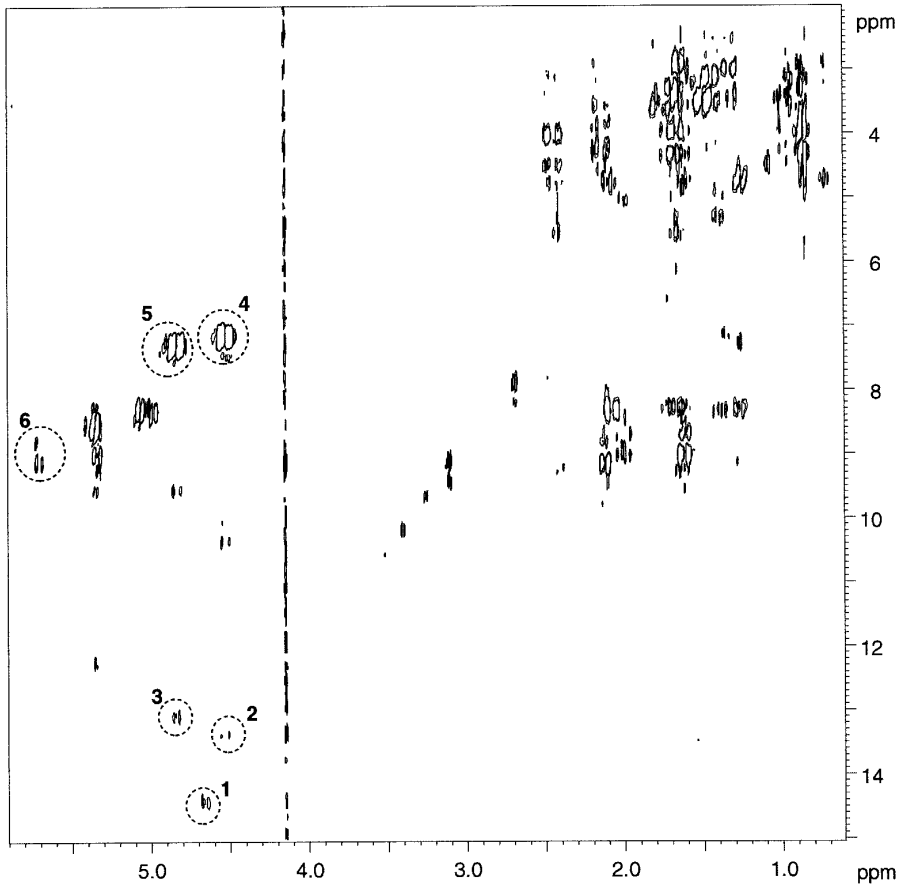

FIG. 5. Two-dimensional spectrum of cyclosporin acquired with the sequence for creation through cross-correlation, and detection through J coupling (Fig. 4). For this particular spectrum, the effective field was tilted by an angle $\theta = 25°$ out of the Oz axis; the mixing time was $\tau_m = 230$ ms. This experiment has been acquired in the phase-sensitive mode through the echo–antiecho procedure. The total acquisition time was about 11 h. The perturbing pulse consists of a 90° hard pulse followed by a strong gradient. The same labeling as in Fig. 3 has been used. One can observe the variation of intensity relative to Fig. 3 and that several cross peaks have disappeared.

then to convert them back by the evolution under the influence of cross-correlation along an effective field axis. Figure 7 shows the $J-\delta$ pulse sequence. For $\theta = 0°$, a similar sequence has been suggested by Bull (*49*), but to the author's knowledge it has never been demonstrated experimentally. The first part of the pulse sequence (until the evolution time t_1) is identical to that of TQS (Fig. 2). The 90° hard pulse which follows the evolution period t_1 allows the conversion of transverse triple-quantum coherences to longitudinal three-spin order. The evolution of the latter may allow the creation of longitudinal one-spin order. Finally the 90° hard pulse converts longitudinal one-spin order into single-quantum transverse coherences which are detected. The 72-step phase cycling of this experiment is obtained by combining the 12-step phase cycling of TQS with a 6-step phase cycling on the third 90° hard pulse which selects the coherence transfer $\Delta p = \pm 3$. As a result of the use of encoding gradients, reduced phase cycling can be used. Phase discrimination in the F1 dimension can be obtained using either the TPPI (*45*) or the States (*50*) schemes as in the TQS sequence. Indeed, the encoding gradients enable only a better selection of the transfer $p = \pm 1$ toward $p = \pm 3$, but the two coherence pathways are simultaneously acquired.

An example of spectrum acquired with the $J-\delta$ sequence is presented in Fig. 8. The interesting feature of this sequence can immediately be noticed. We consider a linear spin network of three spins $I^j-I^k-I^l$ with only $J_{jl} = 0$, and without loss of generality the evolution of transverse coherence of positive number of quanta. We start from I_+^k after the first 90° hard pulse. The density matrix after evolution due to the scalar coupling followed by the second 90° hard pulse contains the triple-quantum coherence term $I_+^j I_+^k I_+^l$, which evolves at the frequency $\omega_j + \omega_k + \omega_l$ during t_1. Converting this triple-quantum transverse coherence into longitudinal three-spin order $I_Z^j I_Z^k I_Z^l$ along the effective field and then letting the system evolve under the influence of relaxation allows the creation of longitudinal one-spin order on each spin I_Z^j, I_Z^k, and I_Z^l. Each coefficient in the density matrix

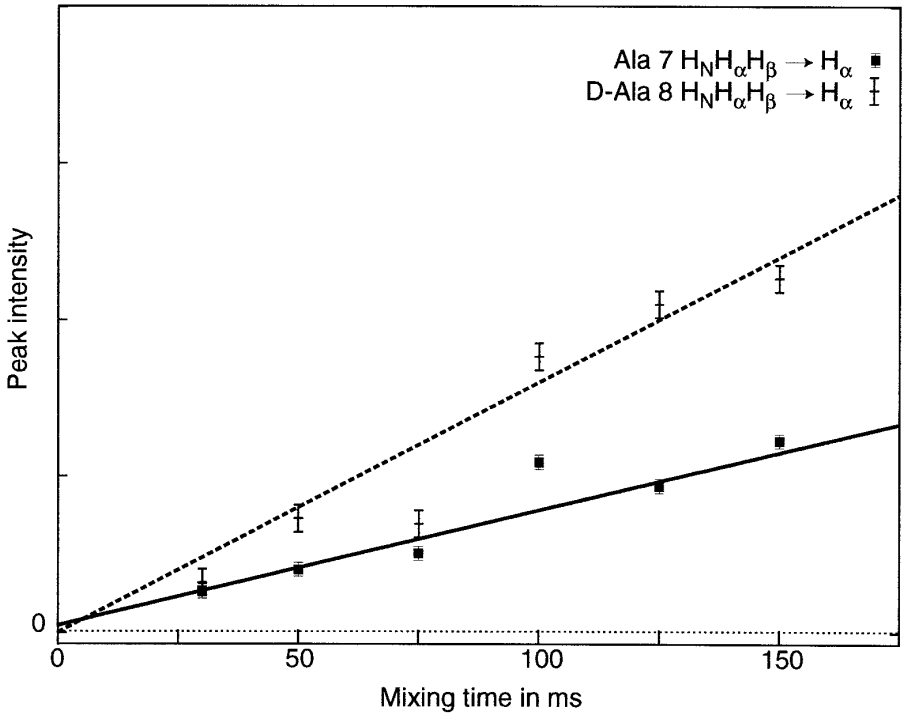

FIG. 6. Examples of buildup curves obtained on the cyclosporin molecule using the sequence for generating through cross-correlation and detection through J coupling (Fig. 4). They correspond to cross peaks labeled **4** and **5.** The angle θ chosen was equal to 0°, and the perturbing pulse was a π pulse. Spectra were acquired in the magnitude mode, and the experiment time was about 4 h per spectrum. The y axis is in arbitrary units. The straight lines have been fitted considering the point (0, 0) and five out of the six experimental points. The choice was based on a comparison among the best-fit χ^2 values. Similar behaviors were observed for other cross peaks. In the linear domain, the slopes are proportional to the sum of the cc-cross-relaxation rates given the three-spin orders considered.

depends on the cc-cross-relaxation rates $\delta_{j,kjl}$, $\delta_{k,jkl}$, and $\delta_{l,jlk}$ respectively. The last 90° hard pulse enables the signal detection. As a consequence, cross peaks at the frequency $(\omega_j + \omega_k + \omega_l, \omega_j)$ are allowed in contrast to the TQS or the $\delta - J$ experiment. Such cross peaks are observed in Fig. 8, as can easily be noticed in the amide proton domain. The peak intensity ratio along a row allows one to compare the relative values of $\delta_{j,kjl}$, $\delta_{k,jkl}$, and $\delta_{l,jlk}$. In the relaxation time domain of linear response and for an isotropic Brownian motion, since the same amount of initial three-spin order is present

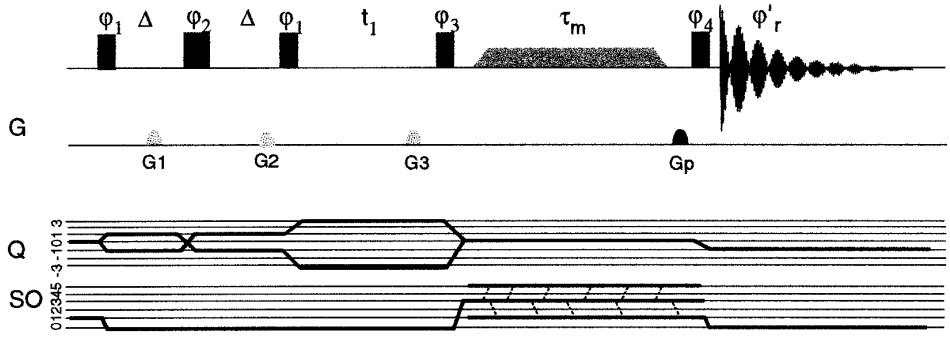

FIG. 7. Pulse sequence used to study in-phase dipole–dipole cross-correlation. The transverse triple-quantum coherences are created through transverse evolution due to scalar coupling and back transformed through evolution under the influence of cross-correlation. The same definitions as previously stated are used. ϕ_3 is equal to 12 × 0°, then 12 × 60°, 12 × 120°, 12 × 180°, 12 × 240°, 12 × 300°. The receiver phase ϕ'_r is 0°, 180°, 0°, 180°, 0°, 180°, 180°, 0°, 180°, 0°, 180°, 0°, 180°, 0°, 180°, 0°, 180°, 0°, 0°, 180°, 0°, 180°, 0°, 180°. Phase-sensitive experiments are obtained by the same manner as that for the TQS experiments. During the mixing time τ_m, self-relaxation and ac- and cc-cross-relaxation from the longitudinal three-spin orders act on the spin system. Only the created one-spin order coherences induce cross peaks with nonvanishing integrals.

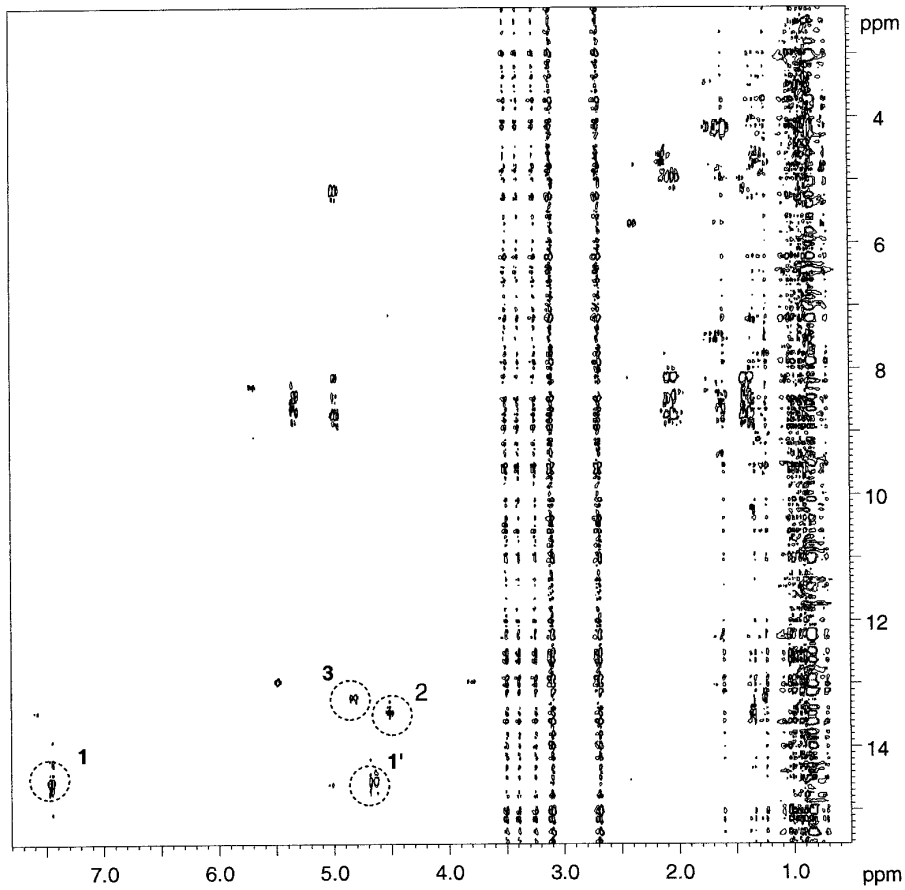

FIG. 8. This spectrum was obtained with the sequence of Fig. 7. The triple-quantum coherences are created by J evolution and back transformed by cross-correlation. For this experiment, we used $\Delta = 25$ ms, $\theta = 15°$ and $\tau_m = 150$ ms. A 180° hard pulse was added after the last 90° hard pulse (see main text). The duration of this experiment was about 55 h. One can observe the appearance of the cross peak **1′** which corresponds to a cross-correlation transfer from $H_N H_\alpha H_\beta$ of Val-5 to H_N. The strong t_1 noise is due to the low receiver gain relative to the intensity of the observed signal.

at $\tau_m = 0$, the cross-peak intensity ratio R of $(\omega_j + \omega_k + \omega_l, \omega_j)$ and $(\omega_j + \omega_k + \omega_l, \omega_k)$ is equal to

$$R = \frac{I_{jkl,j}(\tau_m)}{I_{jkl,k}(\tau_m)} = \frac{(3\cos^2\widehat{\phi_{kjl}} - 1)}{(3\cos^2\widehat{\phi_{jkl}} - 1)} \frac{r_{kl}^3}{r_{jl}^3}. \qquad [23]$$

A careful study of the peak pattern shows that not all cross peaks are in pure absorption in both dimensions. The cancellation of zero-quantum cross peaks will be discussed later, but as mentioned before, since the relevant signals are in-phase, the integration, in the phase-sensitive experiment, circumvents this problem. Finally, while it is difficult with sequences which start by evolution due to cross-correlation ($\delta - J$ or $\delta - \delta$), this sequence can easily be modified to be used in one dimension, by the replacement of the first 90° hard pulse by a selective excitation.

C. Creation and Back Conversion through Cross-Correlation

The last solution consists of the combination of the two relaxation parts of the $\delta - J$ and $J - \delta$ experiments. The $\delta - \delta$ sequence is presented in Fig. 9. After perturbing the density matrix from its thermal equilibrium value by the first hard pulse, the system evolves under the influence of relaxation; cross-correlation allows the creation of all longitudinal odd-spin orders. The 90° hard pulse preceeding the evolution period converts the multispin order into multiquantum transverse coherences. The next 90° hard pulse performs the opposite transformation, and then the system evolves under the influence of relaxation. Finally, the last 90° hard pulse transforms longitudinal one-spin order into transverse single-quantum coherence which can be acquired.

The principle of this experiment can be compared to the 3D NOESY–NOESY experiment (*51*), where the first part (90°–t_1–90°) has been replaced by the perturbing pulse. In the sequence of Fig. 9, one can choose any number of quanta during the t_1 delay. In our case we have chosen the transverse triple-quantum coherences, but the selection of single *and* triple quanta can be performed, giving access to the normalization factor. It is actually not useful, except for clarity reasons, to acquire single- and triple-quantum coherences during t_1, since longitudinal three-spin order $4I_Z^k I_Z^l I_Z^m$ is also

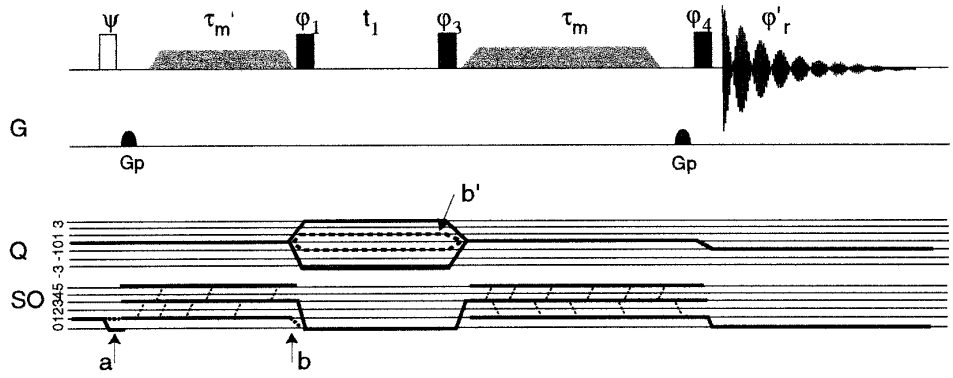

FIG. 9. Pulse sequence to study cross-correlation effects even in the case of vanishing J coupling values; the transverse triple-quantum coherences are created and back converted through evolution under the influence of cross-correlation. τ'_m is the first relaxation period of the sequence. All parameters have the same definitions as those described in the previous figure legends. The *a* arrow points to the spin order pathway as a function of the choice of perturbing pulse (saturation or inversion pulse). The arrows *b* and *b'* show that one can select at the same time the single- and triple-quantum coherences during the evolution time t_1. In the last case, the phases ϕ_1, ϕ_3, and ϕ_r become $\phi_1 = x, -x, -x, x$; $\phi_3 = x, x, x, x, -x, -x, -x, -x$; $\phi_r = x, -x, -x, x, -x, x, x, -x$; and phase-sensitive experiments are obtained by adding 90° to ϕ_1.

transformed by a 90° hard pulse into the single-quantum coherence $4I^k_+I^l_+I^m_-$. As a consequence, a classical 3D NOESY–NOESY experiment contains dipole–dipole cross-correlation information. To our knowledge, such cross peaks have never been reported. But $\theta = 0°$ is not the best angle to study dipole–dipole cc-cross-relaxation in a large protein, a case where the NOESY–NOESY experiment becomes relevant. Experimentally, for the sequence consisting in monitoring the single- and triple-quantum coherences, it is really important to choose a saturation preparation pulse to obtain one-spin order signal on the same order of magnitude as the three-spin order signal. Although we have implemented this saturation pulse, the experimental signal was too weak to obtain quantitative results.

The minimum phase cycling depends on the choice of the quantum number selection during t_1. For triple-quantum selection, one obtains a 72-step phase cycling by the composition of (1) the 12 steps on the 90° hard pulse preceeding the delay t_1, corresponding to the selection of $\Delta p = \pm 3$ (6 steps) and the suppression of axial peaks (factor 2), and (2) the 6 steps for selection of $\Delta p = \pm 3$ on the 90° hard pulse which follows the evolution time t_1. Phase-sensitive experiments can be acquired either in States mode or in TPPI mode by the incrementation of the hard pulse phase preceeding t_1 by 30° from one FID to the next. In principle, this sequence allows the study of cross-correlation between *noncoupled* protons. Indeed, the sequence never requires a nonvanishing J coupling value. The principle of exploitation is identical to that of the $J-\delta$ sequence: a cross peak at the frequency $(\omega_j + \omega_k + \omega_l, \omega_k)$ is proportional (in the time domain of linear response) to the cc-cross-relaxation rate $\sigma^j_{jkl} = \delta_{j,kjl}$.

We have used this sequence with the selection of only the triple-quantum coherences during t_1. As an example, a spectrum is shown in Fig. 10. The global cross-peak patterns are in-phase in both dimensions, although some distortions due to anti-phase single-quantum coherence at $t_2 = 0$ are present, but their effects vanish with signal integration. The cross-peak assignment can be performed. On this spectrum, cross peaks in the amide domain are present, although they were absent in the $\delta-J$ experiments. To improve the experimental conditions of signal acquisition, gradient encoding sequences have been used for the acquisition of this particular spectrum. They allows one to choose a receiver level more adapted to the signal intensity, although, as previously mentioned, the experiments suffer from lack of quantitativity because of the molecular diffusion and selection of only one coherence pathway. We were also able to acquire spectra (not shown) with the $\delta-\delta$ sequence without encoding gradients or with angles θ different from 0°.

V. DISCUSSION

A. Spectral Density Determination

The determination of spectral density functions of biomolecules provides information useful in the comprehension of the molecular recognition processes associated to their biological activity (*17, 18, 52, 53*). Many methods have been proposed, but more measurements are still needed. It would be interesting to explore how spectral density values derived from cross-correlation cross-relaxation rates can be exploited. Some methods have been reported in the heteronuclear case (*11*) for the study of protein side-chain dynamics but none in the homonuclear case. As already mentioned, by measuring these rates at, at least, three angles θ, it is theoretically possible to determine the dipole–dipole cross-correlation spectral density values at three frequencies without any assumption on the motional model. As a test of the consistency of our approach and to explore its capabilities,

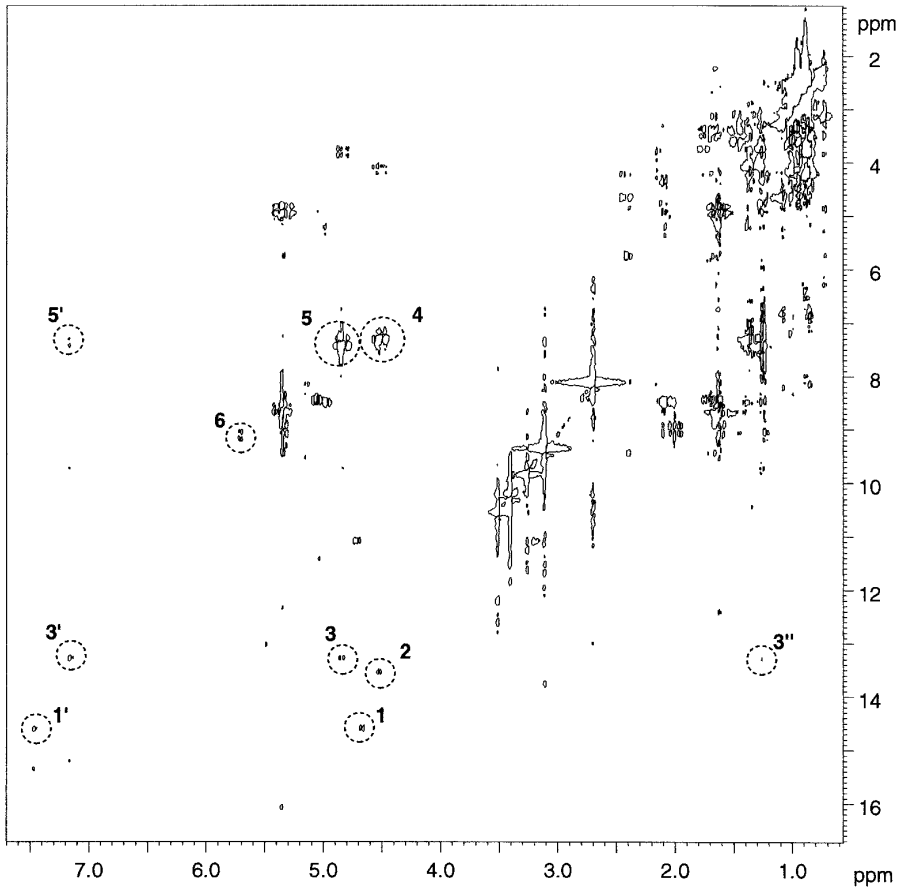

FIG. 10. Spectrum obtained by the sequence of Fig. 9. The transverse triple-quantum coherences are created and detected by cross-correlation. For this particular experiment, we have used encoding gradients before and after the mixing time τ_m. The perturbing pulse was a 180° pulse and the last 90° hard pulse was replaced by a 90° pulse followed by a 180° pulse in quadrature. The angles θ of the two mixing times were equal to 0°. The two durations were $\tau'_m = 250$ ms and $\tau_m = 125$ ms. The total experiment time was about 45 h. The same labels as previously were used. One can observe cross peaks for the amino acid D-Ala-8 at the chemical shift in dimension 1 of $H_N H_\alpha H_\beta$ with a chemical shift in dimension 2 of H_α (peak **3**), but also H_N (peak **3′**) and H_β (peak **3″**). For the amino acid Val-5, only H_N (peak **1′**) and H_α (peak **1**) were observed. The cross peak **5′** corresponds to the chemical shift in dimension F1 of $H_\alpha H_\beta H'_\beta$ and of H_N in dimension F2 of the amino acid D-Ala-8. It may correspond to a spin-diffusion process.

we have recorded a series of spectra at various mixing times and various angles θ. We have used the $\delta - J$ sequence (Fig. 4), since it allows us to obtain spectra in the shortest experiment time. We used nine angles θ from 0 to 60° and two (75 and 150 ms) or three (50, 100, and 150 ms) mixing times. The total number of spectra was 23. Figure 11 shows the initial buildup slope obtained for various cross peaks as a function of the angle θ. We have superimposed two theoretical curves for cross peak $H_\alpha H_\beta H'_\beta \rightarrow H_\alpha$ of the methyl of Leucine 5. For these two curves, we used the angular dependence of the cc-cross-relaxation rate $\delta_{k,lkm}$ (Eq. [10]). The dashed line corresponds to a rigid isotropic molecule and a correlation time of 0.27 ns as derived from off-resonance ROESY measurements. The spectral density functions are thus given by Eq. [19]. The solid line is an adjustment using the theoretical dependence of the cc-cross-relaxation rate $\delta_{k,lkm}$ on the angle θ (Eq. [10]), which implies that $J(0) \sim J(\omega)$ and $J(2\omega) \sim 0$. This experimental result proves that the cc-cross-relaxation rate decreases much faster with the angle θ than would result from the isotropic Brownian rotation. Finally, the study of Fig. 11 reveals that all cross peaks do not exhibit the same behavior as a function of the angle θ, showing that all the cross-correlation spectral density functions are not identical.

It is outside the scope of this article to explore completely the cross-correlation spectral density properties of cyclosporin in $CDCl_3$, but the surprizing behavior of the spectral density function requires comments. Cyclosporin in solution adopts different conformations (*43*). On the other hand, the sequence used measures the sum of the cc-cross-relaxation rates, where each of them may be either positive or negative. It is known that this kind of peptide is rather flexible in solution (*54*) so that the internal dynamics may strongly influence the cross-correlation spectral density functions. The result is that no constraint can be used on theirs signs and magnitudes. It must also be noticed that experimental

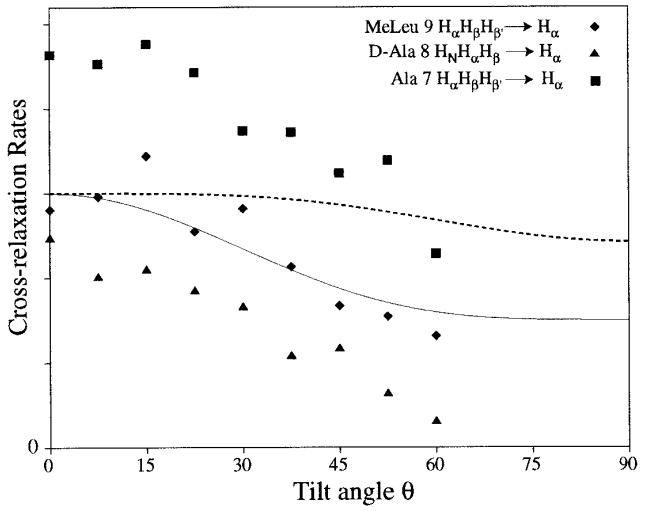

FIG. 11. Variation of the cc-cross-relaxation rates obtained as a function of the angle θ for three different cross peaks (**3, 4,** and **6**). The ordinates are in arbitrary units. Moreover, the rates corresponding to the Ala-7 have been scaled by a factor 1/5. The dashed line corresponds to a correlation time of 0.27 ns assuming an isotropic Brownian motion. The solid line corresponds to a fit using Eq. [10] for the cross-correlation involving the three-spin order on H_α, H_β, and $H_{\beta'}$ of the MeLeu-9 (cross peak **6**). We have chosen for this curve $J(0) = J(\omega)$ and $J(2\omega) = 0$. One can observe that the behavior as a function of the angle θ corresponding to the various cross-correlation cross peaks is different, thus showing the effect of internal dynamics on cross-correlation rates.

bias may be present. Indeed no assessment of the quality of the adiabatic rotations on longitudinal three-spin order coherences has been performed; we simply use the same values as that for the study of longitudinal one-spin order coherence in off-resonance ROESY (*36*). Moreover the absence of ''normalization peaks'' and the increase of self-relaxation but also of cross-relaxation rates with the angle θ (see theoretical section) makes it possible that what we observe does not result from internal dynamics only.

B. Comparison of the Sequences and Possible Improvements

1. Phase of the cross peaks. It can be experimentally noticed that in the $J-\delta$ and $\delta-\delta$ experiments cross peaks are not always purely in-phase. Although these distortions do not prevent the quantification through integration, we have tried various methods to cancel them. First, if the quality of the last 90° hard pulse which preceeds the acquisition is not perfect, it may happen that the longitudinal multispin order coherences are converted into antiphase single-quantum transverse coherences and finally detected. To prevent this, we have modified the two sequences and used a composite 90° hard pulse composed of a 90°–180° sequence where the phase of the π pulse is in quadrature relative to the $\pi/2$ pulse (*34*). An improvement was noticed and the spectra of Figs. 8 and 10 have been acquired with this composite 90° hard pulse. For the cancellation of the always possible zero-quantum cross peaks, we have tried various schemes. Due to a software bug in our spectrometers, the random modulation of the mixing time from one scan to another (*55*) or the accordion method (*56*) induces more noisy spectra when an off-resonance RF irradiation is applied during τ_m, but an improvement in the cancelation of the residual phase distortion in the $J-\delta$ experiment has been noticed. We have also used the method consisting of applying a small B_0 gradient in the presence of a strong on-resonance RF irradiation just after the evolution time (*57*). A real improvement in the cancelation was noticed but associated with a decrease in sensitivity also observed in the case of NOESY experiments.

2. Sensitivity. The major problem with the three sequences is their low sensitivity. If we consider the relaxation rate expressions, cc-cross-relaxation rates are on the same order as ac-cross-relaxation rates for most values of the angle θ. It is true that because of their dependence with the angle $\phi_{\widehat{lkm}}$, some cc-cross-relaxation rates can be vanishingly small, but it is not possible that this should be the case for all of them. We can acquire a reasonably good NOESY spectrum on the cyclosporin sample in about 1 h, but whatever the cross-correlation sequence used, we need an experimental time of at least one order of magnitude longer than that used for NOESY. There are also some intrinsic reasons which explain why the three sequences do not produce results with the same signal-to-noise ratio. Indeed the sequence $\delta-J$ has the great advantage of allowing the use of well-adapted acquisition gain level due to the gradient filtering just before the acquistion. The same technique could be used for the $J-\delta$ and $\delta-\delta$ sequences, but the experimental results suffer from the signal loss by molecular diffusion in the case of cyclosporin in chloroform at room temperature. The second inherent difficulty is related to the conversion of transverse triple-quantum into three-spin order coherences. Only 1/4 of the magnetization is converted; the same factor is, in fact, present for the TQF-NOESY and TQF-ROESY experiments. The last remark concerns the possible magnetization loss by relaxation during the evolution time t_1, since we consider the transverse evolution of triple-quantum coherences. It turns out that our experiments do not suffer from this, because of the large spectral width and the small number of t_1 values used. However a careful study shows that these intrinsic reasons are not sufficient to explain the low signal. A comparison of experimental signals between a cross-relaxation and a cross-correlation experiments shows that a factor of about 40 is missing in the latter, which reduces to about one order of magnitude when the 1/4 factor, as described above, is taken into account. A possible reason could be the large flexibility of the cyclosporin at room temperature, which averages out the cc-cross-relaxation rates much faster than the ac-cross-relaxation rates through the fluctuation of the angle $\phi_{\widehat{lkm}}$.

VI. CONCLUSION

In this article, we have described three schemes to explore cross-correlation along an effective field axis. The concept is based on the measurement of multiquantum transverse magnetization during the evolution time. Although we have made all experimental developments for the case of dipole–dipole cross-correlation, the case of CSA/DD or dipole–dipole involving a paramagnetic spin (*47*) can be treated by the same approach. The major advantages of these sequences relative to the previous schemes (DQF-NOESY, TQF-NOESY, and TQF-ROESY) reside in a simple assignment proceedure and in the fact that the relevant peaks are in-phase in both dimensions, allowing one to eliminate zero-quantum cross peaks through integration. This enables a quantification of these triple-quantum peaks relative to the single-quantum peaks for the scheme $(\delta-\delta)$, for which there is no restriction on the coupling network. Finally, the three schemes allow the exploration of the cross-correlation spectral density function by varying the angle θ. However, the most powerful sequences suggested ($J-\delta$ and $\delta-\delta$) suffer from a lack of sensitivity for intrinsic reasons (selection of high order transverse magnetization and conversion into high order longitudinal spin order) but it seems also to be affected by internal dynamics. Our first dynamic results tend to prove that dipole–dipole cross-correlation is averaged out more efficiently than ac-cross-relaxation by the internal dynamics, probably due to fluctuations of $\phi_{\widehat{jkl}}$. A complete investigation of a molecule exhibiting dynamics which can be more easily described than the cyclosporin molecule is therefore desirable. Finally the proposed schemes make it possible to explore experimentally the relaxation dynamics of longitudinal multispin order. As theoretically shown, the study of their relaxation is not easy because the self-relaxation and the cross-relaxation rates increase with the number of spins involved in the coherence.

ACKNOWLEDGMENTS

The author is indebted to Professor G. Bodenhausen for having stimulated this work, to Dr. B. Boulat for many useful discussions and for the acquisition of spectra on the Varian spectrometer, and to Professor M. Goldman and Dr. V. Fazakerley for a careful reading of the manuscript. N.H.M.F.L. and the CEA are acknowledged for financial support.

REFERENCES

1. A. Abragam, ''Principles of Nuclear Magnetism,'' Clarendon Press, Oxford (1961).
2. H. M. McConnell, *J. Chem. Phys.* **25,** 709 (1956).
3. J. H. Freed and G. K. Fraenkel, *J. Chem. Phys.* **39,** 326 (1963).
4. E. L. Mackor and C. MacLean, *J. Chem. Phys.* **44,** 64 (1966).
5. R. Wilson and D. Kivelson, *J. Chem. Phys.* **44,** 154 (1966).
6. J. S. Blicharski, *Phys. Lett. A* **24,** 608 (1967).
7. L. G. Werbelow and D. M. Grant, *J. Chem. Phys.* **63,** 544 (1975).
8. M. Goldman, *J. Magn. Reson.* **60,** 437 (1984).
9. J. Brondeau, D. Canet, C. Millot, H. Nery, and L. Werbelow, *J. Chem. Phys.* **82,** 2212 (1985).
10. J. Boyd, U. Hommel, and I. Campbell, *Chem. Phys. Lett.* **175,** 477 (1990).
11. M. Ernst and R. R. Ernst, *J. Magn. Reson. A* **110,** 202 (1994).
12. N. Tjandra, A. Szabo, and A. Bax, *J. Am. Chem. Soc.* **118,** 6986 (1996).
13. M. Guéron, J. L. Leroy, and R. H. Griffey, *J. Am. Chem. Soc.* **105,** 5811 (1982).
14. T. C. Farrar and R. A. Quintero-Arcaya, *J. Phys. Chem.* **91,** 3224 (1987).
15. S. Wimperis and G. Bodenhausen, *Mol. Phys.* **66,** 897 (1989).
16. A. G. Palmer III, N. J. Skelton, W. J. Chazin, P. E. Wright, and M. Rance, *Mol. Phys.* **75,** 699 (1992).
17. J. W. Peng and G. Wagner, *J. Magn. Reson.* **98,** 308 (1992).
18. L. E. Kay, L. K. Nicholoson, F. Delaglio, A. Bax, and D. A. Torchia, *J. Magn. Reson.* **97,** 359 (1992).
19. K. T. Dayie and G. Wagner, *J. Magn. Reson. A* **111,** 121 (1996).
20. C. Dalvit and G. Bodenhausen, *Chem. Phys. Lett.* **161,** 555 (1989).
21. C. Dalvit and G. Bodenhausen, *J. Am. Chem. Soc.* **110,** 7924 (1988).
22. T. E. Bull, *J. Magn. Reson.* **93,** 596 (1991).
23. T. E. Bull, *Prog. NMR Spectrosc.* **24,** 377 (1992).
24. R. Brüschweiler, C. Griesinger, and R. R. Ernst, *J. Am. Chem. Soc.* **111,** 8034 (1989).
25. G. Jaccard, S. Wimperis, and G. Bodenhausen, *Chem. Phys. Lett.* **138,** 601 (1987).
26. T. C. Farrar and I. C. Locker, *J. Chem. Phys.* **87,** 3281 (1987).
27. Gy. Batta and J. Gervay, *J. Am. Chem. Soc.* **117,** 368 (1995).
28. I. Burghardt, R. Konrat, and G. Bodenhausen, *Mol. Phys.* **75,** 467 (1992).
29. V. Varmar, N. D. Kurur, and G. Bodenhausen, *J. Magn. Reson. A* **118,** 64 (1996).
30. T. Meersman, M. Schwager, V. Varma, and G. Bodenhausen, *J. Magn. Reson. A* **119,** 275 (1996).
31. M. Karplus, *J. Chem. Phys.* **30,** 11 (1959).
32. R. A. Venters, W. J. Metzler, L. D. Spicer, L. Mueller, and B. T. Farmer II, *J. Am. Chem. Soc.* **117,** 9592 (1996).
33. S. Grzesiek, P. Wingfield, S. Stahl, J. D. Kaufman, and A. Bax, *J. Am. Chem. Soc.* **117,** 9594 (1996).
34. R. R. Ernst, G. Bodenhausen, and A. Wokaun, ''Principles of Nuclear Magnetic Resonance in One and Two Dimensions,'' Clarendon Press, Oxford (1987).
35. M. Goldman, ''Quantum Description of High-Resolution NMR in Liquids,'' Clarendon Press, Oxford (1987).
36. H. Desvaux, P. Berthault, N. Birlirakis, M. Goldman, and M. Piotto, *J. Magn. Reson. A* **113,** 47 (1995).
37. H. Desvaux, P. Berthault, N. Birlirakis, and M. Goldman, *J. Magn. Reson. A* **108,** 219 (1994).
38. H. Desvaux, C. Wary, N. Birlirakis, and P. Berthault, *Mol. Phys.* **86,** 1048 (1995).
39. A. R. Edmons, ''Angular Momentum in Quantum Mechanics,'' Princeton Univ. Press, Princeton (1960).
40. L. G. Werbelow and A. G. Marshall, *Mol. Phys.* **28,** 113 (1974).
41. H. Desvaux, P. Berthault, and N. Birlirakis, *Chem. Phys. Lett.* **233,** 545 (1995).

42. H. Kesler, H.-R. Loosli, and H. Oskinat, *Helv. Chim. Acta* **68,** 661 (1985).

43. S. W. Fesik, R. T. Gampe Jr., H. L. Eaton, G. Gemmecker, E. T. Olekniczak, P. Neri, T. F. Holzman, D. A. Egan, R. Edalji, R. Simmer, R. Helfrich, J. Hochlowski, and M. Jackson, *Biochemistry* **30,** 6574 (1991).

44. J. Stonehouse, P. Adell, J. Keeler, and A. J. Shaka, *J. Am. Chem. Soc.* **116,** 6037 (1994).

45. D. Marion and K. Wüthrich, *Biochem. Biophys. Res. Commun.* **113,** 967 (1983).

46. N. Müller, G. Bodenhausen, and R. R. Ernst, *J. Magn. Reson.* **75,** 297 (1987).

47. H. Desvaux, M. Gochin, and G. Bodenhausen, to be published.

48. J.-M. Böhlen, S. Wimperis, and G. Bodenhausen, *J. Magn. Reson.* **77,** 589 (1988).

49. T. E. Bull, *J. Magn. Reson.* **72,** 397 (1987).

50. D. J. States, R. A. Haberkorn, and D. J. Reuben, *J. Magn. Reson.* **48,** 286 (1982).

51. T. A. Holak, J. Habazettl, H. Oschkinat, and J. Otlewski, *J. Am. Chem. Soc.* **113,** 3196 (1991).

52. R. Brüschweiler and D. A. Case, *Prog. NMR Spectrosc.* **26,** 27 (1994).

53. J. W. Peng and G. Wagner, *Biochemistry* **34,** 16733 (1995).

54. R. Brüschweiler, M. Blackledge, and R. R. Ernst, *J. Biomol. NMR* **1,** 3 (1991).

55. S. Macura, Y. Huang, D. Suter, and R. R. Ernst, *J. Magn. Reson.* **43,** 259 (1981).

56. S. Macura, K. Wüthrich, and R. R. Ernst, *J. Magn. Reson.* **46,** 269 (1982).

57. A. L. Davis, G. Estcourt, J. Keeler, E. D. Laue, and J. J. Titman, *J. Magn. Reson. A* **105,** 167 (1993).